

## Short Communication

# Selective benzylic oxidation of alkylaromatics over Cu/SBA-15 catalysts under solvent-free conditions



Chinna Krishna Prasad Neeli, Anand Narani, Ravi Kumar Marella, Kamaraju Seetha Rama Rao, David Raju Burri\*

Catalysis Laboratory, Indian Institute of Chemical Technology, Hyderabad-500007, India

## ARTICLE INFO

## Article history:

Received 12 March 2013

Received in revised form 27 April 2013

Accepted 29 April 2013

Available online 6 May 2013

## Keywords:

Cu/SBA-15

Benzylic oxidation

Ethylbenzene

Acetophenone

## ABSTRACT

With the purpose of benzylic oxidation of alkylaromatics into corresponding ketones selectively under solvent-free conditions, cheap, simple and versatile Cu/SBA-15 catalyst system with the Cu loading of 5, 10, 15 and 20% has been prepared by impregnating SBA-15 support. Among Cu/SBA-15 catalysts, 10%Cu/SBA-15 exhibited superior activity and selectivity.

© 2013 Elsevier B.V. All rights reserved.

## 1. Introduction

Ketones and aldehydes are important intermediates in the pharmaceutical and fine-chemical industries, particularly in the production of flavors, fragrances, and biologically active compounds [1]. Benzylic oxidation of alkylaromatics is one of the important methods for the production of ketones and aldehydes, wherein, potassium permanganate and potassium dichromate are the generally used oxidants in stoichiometric or excess quantities [2,3], which leads to large amount of toxic waste. Development of oxidation methods using a catalytic amount of metal reagent and an appropriate amount of oxidant is the subject of interest. With this intention, in the last decade, various catalytic methods are investigated using metal complexes of Cr, Co, Mn, Rh, Ru, Zn, Fe etc. [4–16]. However, toxicity, high cost, waste disposal and removal of residual metal from the product are some of inherent problems still to be resolved. Some of the above cited problems associated with the homogeneous metal complex catalysts can be resolved in heterogeneous catalytic systems.

Of late, mesoporous silica materials like MCM-41, TUD-1 and SBA-15 have attracted considerable attention as promising new hydrocarbon oxidation carriers [17]. Benzylic oxidation of ethylbenzene to acetophenone over Ti/MCM-41, V/MCM-41 and Cr/MCM-41 catalysts is reported with 12% conversion of ethylbenzene and 83% selectivity of acetophenone [18]. Recently, SBA-15 supported cobalt catalysts are reported with different oxidants [19]. In one of our recent report, highly active SBA-15 supported silver catalysts are reported [20]. There are few

reports on copper containing heterogeneous catalytic systems, wherein, moderate conversions and selectivities are obtained [21–25], which are cost ineffective and involvement of carcinogenic solvents.

Herein, a highly efficient and cheap Cu/SBA-15 catalyst system towards the benzylic oxidation of alkylaromatics into corresponding ketones under solvent-free conditions is reported.

## 2. Experimental methods

### 2.1. Catalyst preparation

SBA-15 support was synthesized according to original report of Zhao et al. [26] and our previous publications [27–30]. The calcined (at 823 K for 8 h) SBA-15 support was dried at 423 K for 6 h and impregnated with the requisite amounts of aqueous  $\text{Cu}(\text{NO}_3)_2 \cdot 3\text{H}_2\text{O}$  solution likely to be around 5, 10, 15, 20 wt.% as Cu metal. Subsequently catalyst samples were dried at 393 K for 12 h and calcined at 723 K for 6 h, reduced at 553 K for 3 h in  $\text{H}_2$  flow and denoted as xCu/SBA-15 where x indicates the percentage (by weight) loading of Cu on SBA-15 support.

### 2.2. Catalyst characterization

XRD patterns were obtained from Ultima-IV (M/s. Rigaku Corporation, Japan) diffractometer with a nickel filtered  $\text{CuK}\alpha$  radiation. The  $\text{N}_2$  adsorption–desorption isotherms were measured by Quadrasorb-SI V 5.06 (M/s. Quantachrome Instruments Corporation, USA). TPR experiments were conducted using a home-made TPR system [30]. The XPS analysis was made on a photoelectron spectrometer (KRATOS Axis 165, Shimadzu, Japan) with  $\text{Mg K}\alpha$  radiation (1253.6 eV).

\* Corresponding author. Tel.: +91 40 27193232; fax: +91 40 27160921.

E-mail address: [david@iict.res.in](mailto:david@iict.res.in) (D.R. Burri).

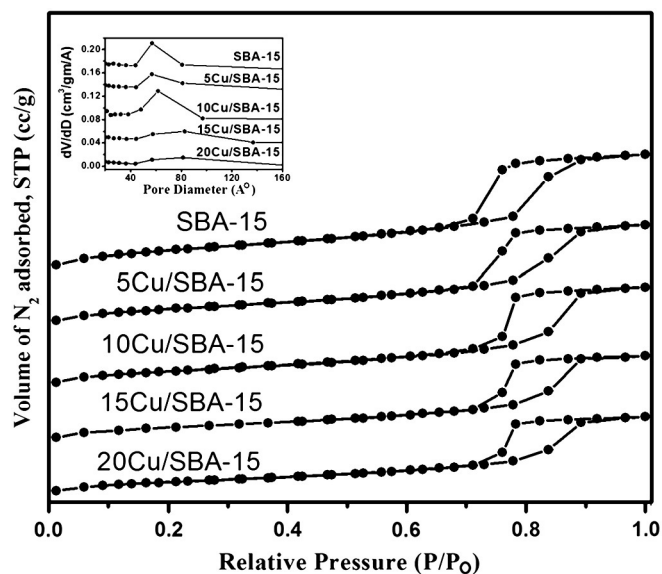


Fig. 1.  $N_2$  adsorption–desorption isotherms of Cu/SBA-15 catalyst (pore size distribution curves as inset).

### 2.3. Catalytic activity tests

Typically, 50 mg of catalyst, 1 mmol of substrate, and 3 mmol of 70% *t*-BuOOH (Sigma Aldrich) were taken in a RB flask and constantly stirred at 363 K for 5 h under solvent-free conditions. Unless otherwise specified the above reaction conditions are applicable. The catalyst was separated by filtration and analyzed by GC (GC-17A model, M/s. Shimadzu Instruments, Japan) consisting of FID and OV-1 capillary column (0.53 mm  $\times$  30 m) using toluene as external standard. The product identification was made by GC-MS (QP5050 model, M/s. Shimadzu Instruments, Japan) consisting of DB-5 column (0.32 mm dia. and 25 m long, M/s. J & W Scientific, USA). The separated catalyst was washed with methanol and dried under vacuum prior to reuse.

## 3. Results and discussion

### 3.1. Catalyst characterization

As shown in Fig. 1, the  $N_2$  adsorption–desorption isotherms of parent mesoporous SBA-15 and Cu/SBA-15 catalysts are of type IV and exhibited H1 hysteresis loops in accordance with the IUPAC classification, revealing the retention of porous texture of parent SBA-15 in all the Cu/SBA-15 catalysts. In general, the total pore volume decreases

**Table 1**  
Structural and textural parameters of Cu/SBA15 catalysts.

Catalyst	$S_{BET}$ ( $m^2/g$ ) <sup>a</sup>	$V_t$ ( $cm^3/g$ ) <sup>b</sup>	$D_{BJH}$ (nm) <sup>c</sup>	$d_{100}$ (nm) <sup>d</sup>	$a_0$ (nm) <sup>e</sup>	$t$ (nm) <sup>f</sup>	Cu (wt.%) <sup>g</sup>
SBA-15	925	1.188	5.68	8.66	10.00	4.32	–
5Cu/SBA-15	816	1.496	7.89	8.91	10.28	2.39	4.95
10Cu/SBA-15	719	1.371	6.16	8.91	10.28	4.12	9.84
15Cu/SBA-15	623	1.184	8.26	9.03	10.43	2.17	13.76
20Cu/SBA-15	567	1.080	8.15	8.57	9.90	1.75	18.92

<sup>a</sup> BET surface area.

<sup>b</sup> Total pore volume.

<sup>c</sup> BJH average pore diameter.

<sup>d</sup> Periodicity of (100) plane.

<sup>e</sup> Unit cell length ( $a_0 = 2d_{(100)} / \sqrt{3}$ ).

<sup>f</sup> Pore wall thickness ( $t = a_0 - D_{BJH}$ ).

<sup>g</sup> Cu% determined by AAS.

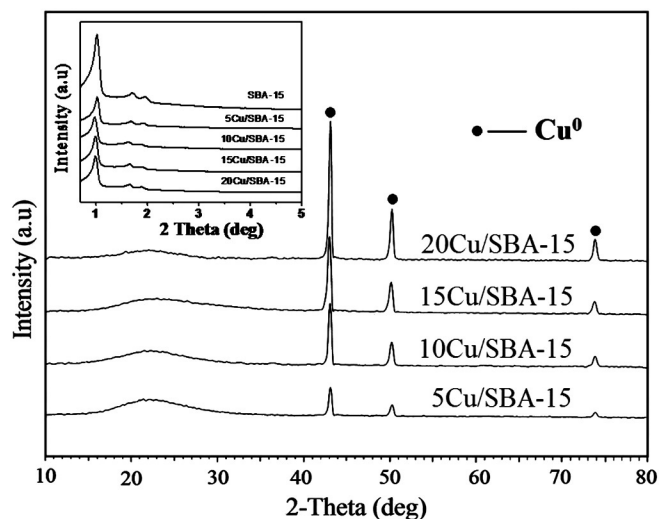


Fig. 2. XRD patterns of Cu/SBA-15 catalysts and their low-angle XRD patterns as inset.

as the loading of active component increases. Contrarily, the total pore volume of 5Cu/SBA-15 is more than that of parent SBA-15. The additional pore volume of Cu/SBA-15 catalysts may be the contribution of CuO species, which is expected from the metal support interaction. The discrepancies in the pore diameter and pore wall thickness are indicating the metal support interaction. The structural and textural parameters and pore size distributions can be found from Table 1 and Fig. 1 inset respectively. The low-angle XRD patterns (Fig. 2 inset) are consistent with the reported literature [26]. Fig. 2 shows three sharp

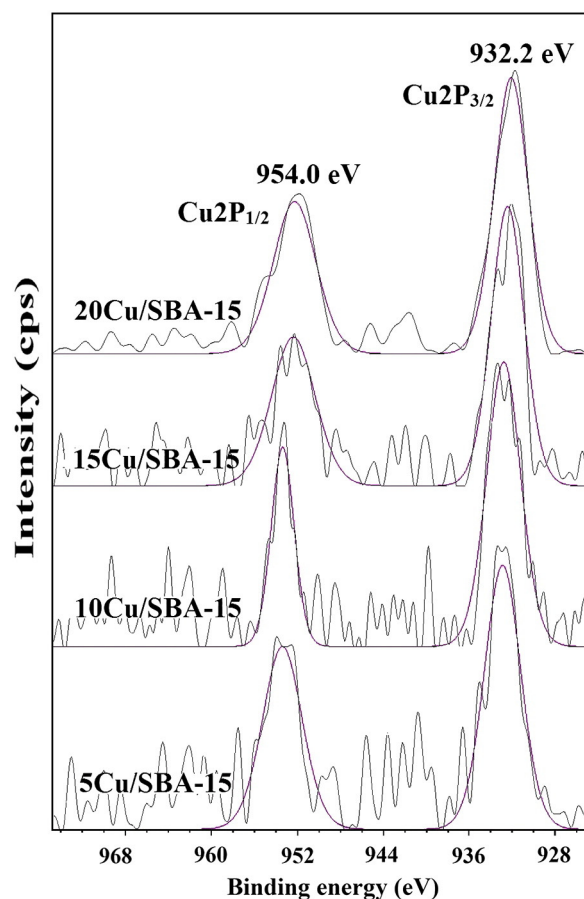


Fig. 3. XPS spectrum of Cu/SBA-15 catalysts.

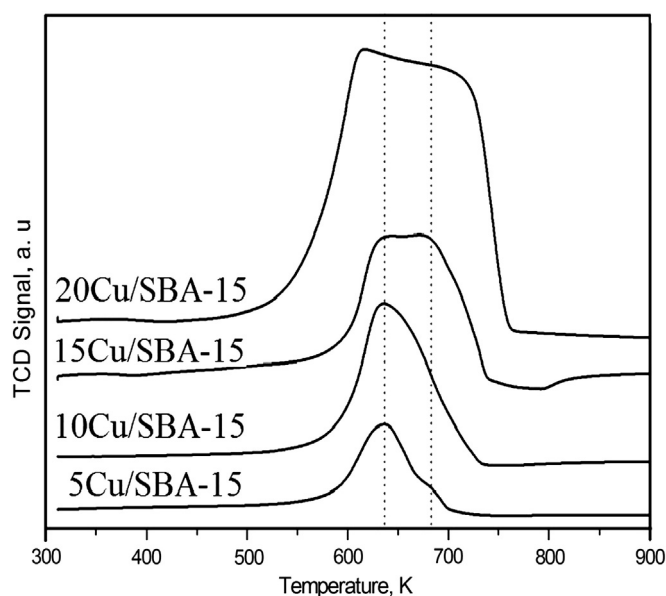


Fig. 4. TPR patterns of CuO/SBA-15 catalysts.

XRD peaks at 43.6, 50.8, and 74.4° on  $2\theta$  scale, corresponding to (111), (200), and (220) planes of metallic copper in accordance with the JCPDS card No. 04-0836. Appearance of an intense and broad photoelectron peak in Fig. 3 at the binding energies of 932.2 eV ( $\text{Cu}2p_{3/2}$ ) and  $\text{Cu}2p_{1/2} = 954$  eV and absence of  $2p \rightarrow 3d$  satellite peak indicate the existence of copper species either in  $\text{Cu}^0$  or  $\text{Cu}^+$ , which is in agreement with the reported literature [31]. Assessing the reduction behavior of  $\text{Cu}^{2+}$  species that supported on SBA-15 has been investigated by a well known and a valid TPR technique. The  $\text{H}_2$ -TPR profiles of calcined Cu/SBA-15 catalysts are displayed in Fig. 4. From the reduction profile of 5Cu/SBA-15 catalyst two reduction peaks can be observed, where a main reduction peak appeared at 635 K due to reduction of CuO to  $\text{Cu}^0$  or metallic Cu species ( $\text{CuO} + \text{H}_2 \rightarrow \text{Cu} + \text{H}_2\text{O}$ ) in a single stage and a shoulder peak that appears at 680 K may be due to reduction of  $\text{Cu}^{1+}$  species into metallic Cu ( $\text{Cu}_2\text{O} + \text{H}_2 \rightarrow 2\text{Cu} + \text{H}_2\text{O}$ ). In the case of 10Cu/SBA-15 catalyst, only a single reduction peak is

Table 2

Effect of Cu loading on the oxidation of ethylbenzene over Cu/SBA-15 catalysts at 363 K for 5 h using t-BuOOH as oxidant under solvent free conditions.

Catalyst	Crystallite size (nm) <sup>a</sup>	EB conversion (%) <sup>b</sup>	ACP selectivity (%) <sup>c</sup>
5Cu/SBA-15	25.02	82	95.8
10Cu/SBA-15	30.81	94	99.0
15Cu/SBA-15	43.54	86	97.6
20Cu/SBA-15	49.55	85	96.5
No catalyst	–	30	100
SBA-15	–	32	100
CuO	–	36	95.4
10CuO/SBA-15	–	40	96.0
10Cu/SiO <sub>2</sub>	–	60	51.0

<sup>a</sup> Determined from Scherrer equation.

<sup>b</sup> EB = ethylbenzene.

<sup>c</sup> ACP = acetophenone.

Table 3

Effect of 10Cu/SBA-15 catalyst amount on activity at 363 K for 5 h with t-BuOOH under solvent-free conditions.

Catalyst weight (mg)	EB conversion (%)	ACP selectivity (%)	BZD selectivity (%)
25	85	97.5	2.5
50	94	99.0	1.0
75	91	98.2	1.8
100	90	97.8	2.2

Table 4

Effect of reaction temperature on activity of 10Cu/SBA-15 for 5 h with t-BuOOH under solvent-free conditions.

Temperature, K	EB conversion (%)	ACP selectivity (%)	BZD selectivity (%)
300	27	75	25
323	48	86	14
363	94	99	01
373	95	92	08

Table 5

Effect of reaction time on activity of 10Cu/SBA-15 at 363 K with t-BuOOH under solvent-free conditions.

Time, h	EB conversion (%)	ACP selectivity (%)	BZD selectivity (%)
1	38	94.0	6.0
2	51	95.5	4.5
3	65	96.7	3.3
4	83	98.4	1.6
5	94	99.0	1.0
6	94	97.8	2.2

observed at 635 K, which corresponds to the reduction of  $\text{Cu}^{2+}$  species into metallic Cu. The TPR results of 10Cu/SBA-15 catalyst are consistent as reported by Zhu et al., over Cu/SiO<sub>2</sub> catalyst, where appearance of one single reduction peak is the manifestation of uniformly dispersed CuO particles [32]. The shift in the reduction temperature to lower values with increase in Cu loading may be due to attainment of bulk nature of CuO species [33]. A second reduction peak that appears at higher temperature (680 K) in all the other Cu/SBA-15 catalysts may be the reduction of CuO species that aggregated outside the pores [34]. The results reveal that the interaction between CuO and SBA-15 support increases with Cu loading and the CuO species are getting aggregated both in pores and on the external surface of SBA-15 support.

Table 6

Effect of oxidant on activity of 10Cu/SBA-15 catalyst at 363 K for 5 h under solvent-free conditions.

Oxidant	EB conversion (%)	ACP selectivity (%)	BZD selectivity (%)
50 wt.% aq.H <sub>2</sub> O <sub>2</sub>	86	52	48
90 wt.% urea H <sub>2</sub> O <sub>2</sub>	80	74	26
O <sub>2</sub> (1 atm)	–	–	–
70% TBHP	94	99	1.0

Table 7

Effect of t-BuOOH concentration on activity of 10Cu/SBA-15 at 363 K for 5 h under solvent-free conditions.

BuOOH (mmol)	EB conversion (%)	ACP selectivity (%)	BZD selectivity (%)
1	50	93.5	6.5
2	85	97.6	2.4
3	94	99.0	1.0
4	92	98.2	1.8

Table 8

Effect of solvent (2 ml) on activity of 10Cu/SBA-15 catalyst at 363 K for 5 h with t-BuOOH.

Solvent	EB conversion (%)	ACP selectivity (%)	BZD selectivity (%)
MEOH	12	88.3	11.7
Water	20	85.5	14.5
Dichloroethane	28	82.6	17.4
Toluene	72	84.2	15.8
Acetonitrile	86	92.0	8.0
No solvent	94	99.0	1.0

**Table 9**  
Activity of 10Cu/SBA-15 at different stirring rates.

Rpm	Conversion (%)	Selectivity to ACP (%)	Selectivity to BZD (%)
500	93.6	98.52	1.48
600	93.4	98.34	1.66
700	94.2	99.16	0.94
800	94.3	99.03	0.97

**Table 10**  
Activity of 10Cu/SBA-15 catalyst at different particle sizes.

Mesh range	Conversion (%)	Selectivity to ACP (%)	Selectivity to BZD (%)
16–18	94.36	99.10	0.90
18–30	93.95	98.73	1.27
30–72	93.84	98.94	1.06
40–60	93.87	98.87	1.13

**Table 11**  
Recyclability of 10Cu/SBA-15 for benzylic oxidation of ethylbenzene.

Recyclability	Conversion (%)	Selectivity to ACP (%)	Selectivity to BZD (%)
Fresh	94	99.0	1.0
Cycle-1	94	99.2	0.8
Cycle-2	94	99.1	0.9
Cycle-3	94	98.8	1.2

### 3.2. Benzylic oxidation of ethylbenzene

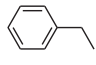
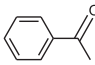
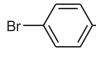
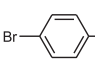
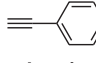
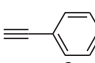
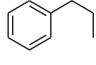
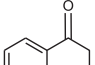
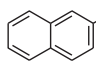
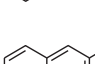
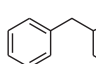
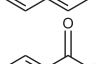
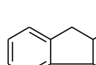
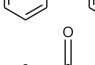
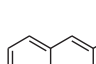
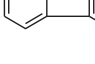
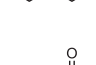
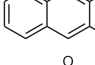
In general, ethylbenzene (EB) oxidation leads to several products viz., 1-phenylethanol (1-PhE), benzaldehyde (BZD), acetophenone (ACP), 2-phenylethanol (2-PhE), phenyl acetaldehyde (PhACD), etc. [35]. However, Cu/SBA-15 catalysts with aqueous t-BuOOH under solvent-free conditions selectively oxidized to ACP and BZD, where ACP is the main product, which occurs through benzylic oxidation.

To maximize the yield of ACP via benzylic oxidation various reaction parameters have been optimized. Table 2 shows that the optimum loading of Cu is 10%, i.e., 10Cu/SBA-15 catalyst. Hence, further activity studies are made using 10Cu/SBA-15 as a catalyst. The amount of catalyst optimized [36] was found to be 50 mg of 10Cu/SBA-15 catalyst (Table 3). The influence of reaction temperature over 10Cu/SBA-15 catalyst is displayed in Table 4, which reveals that the optimum reaction temperature is 363 K. According to Table 5, the optimum reaction time is 5 h. From Table 6, 70% t-BuOOH is the best oxidant. Table 7 indicates that the optimum t-BuOOH to EB ratio is 3:1. Table 8, reveals the superiority of solvent-free system. The data presented in Tables 9 and 10 reveals the absence of any mass transfer limitations. 10Cu/SBA-15 catalyst is used in three repeated cycles (Table 11) and no significant

**Table 12**  
Comparison of figure of merit of the present work with other studies in the literature.

Catalyst	Oxidant	Reaction time (h)	T (°C)/solvent	EB conversion (%)	Selectivity (%)			Ref.
					ACP	BZD	Others	
Polymer anchored Cu(II)	TBHP	6	60/acetonitrile	44	97	–	3	[3]
ZeoliteY Cu(II) complex	TBHP	10	60/acetonitrile	37	97	–	3	[6]
YCu-fsal complex	H <sub>2</sub> O <sub>2</sub>	8	70/benzene	65	100	–	–	[7]
Si/Al-pr-NH-et-N methyl-2-pyridylketone-Mn	TBHP	24	80/–	67	93	2.7	4	[8]
CuTUD-1	TBHP	5	80/acetonitrile	35	67	10.3	23	[9]
Cr/MCM41	TBHP	12	60/methanol	88	85	–	15	[10]
Co/MCM-41	TBHP	24	–	26	85	–	15	[12]
Co/SBA15	TBHP	24	80/acetonitrile	38	83	–	18	[15]
Mn/SBA15	TBHP	8	–	25	37	–	63	[17]
Ag/SBA15	TBHP	5	–	92	99	–	1	[18]
Cu/SBA15	TBHP	5	–	94	>99	–	<1	Present work

**Table 13**  
Benzylic oxidation of alkyl aromatics over 10Cu/SBA-15 catalyst under solvent-free conditions.

S. no.	Substrate	Product	Conv. (%)	Sel. (%)
1			94	99
2			90	97
3			85	96
4			95	98
5			91	94
6			96	98
7			98	99
8			48	82
9			42	84

Reaction conditions: Catalyst = 50 mg, substrate = 1 mmol, t-BuOOH = 3 mmol, temp. = 363 K, time = 5 h.

loss in activity is observed. However, it is essential to wash and reduce the catalyst prior to reuse.

The oxidation of EB over 10Cu/SBA-15 catalyst has been compared with the other catalysts reported in the literature in Table 12. Compared to SBA-15 supported Cu catalysts, polymer supported and zeolite supported catalysts are inferior due to the presence of copper as Cu<sup>2+</sup>. Mesoporous silica supported Mn, Cr and Co catalysts are reported for the benzylic oxidation of ethylbenzene. However these catalysts are inferior compared to Cu/SBA-15 catalyst, the details are presented elsewhere (Table 12).

Evaluating the scope of 10Cu/SBA-15 catalyst for the benzylic oxidation of various alkylaromatics along with EB is presented in Table 13, which reveals that the conversion and the selectivities of several alkylaromatics (Entries 2–7) are more or less equal to that



of EB, whereas in the case of 2-ethylanthracene (Entry 8) and 2-ethylanthracene-9, 10-dione (Entry 9), both conversions and selectivities are moderate. The enhanced activity towards benzylic oxidation is observed in the case of certain molecules such as diphenylmethane (Entry 6) and 9H-fluorene (Entry 7), where a benzylic carbon is being shared by two benzyl groups. Contrarily, diminishing activity of the catalyst is observed as the number of fused rings increases (Entries 1, 5 and 8). To sum up the catalytic activity order is as follows, ethylbenzene > ethylnaphthalene > ethylanthracene.

The textural features of hexagonally ordered mesoporous SBA-15 seem to play a crucial role in the benzylic oxidation of alkylaromatics. High surface area (925 m<sup>2</sup>/g) of SBA-15 support may provide ample space for the deposition and stabilization of active Cu metal nanoparticles. The ordered mesopores of SBA-15 act as micro-reactors and the deposited Cu metal particles in and around microporous corona act as reactive centers. Since the adsorption of reactants followed by surface reaction and desorption of products takes place in the mesopores of Cu/SBA-15, the diffusion limitations are expected to be minimized. During the transportation of reactants in the confined environment (mesopores), high accessibility with the active Cu sites occurs, which leads to high activity of the catalyst. On the whole, the textural characteristics of mesoporous SBA-15 support assist for the active copper species stabilization and providing accessibility to the reactants collectively responsible for higher conversion and selectivity of Cu/SBA-15 catalysts.

#### 4. Conclusion

In summary, 10Cu/SBA-15 catalyst is found to be an efficient catalyst for the benzylic oxidation of alkylaromatics into corresponding ketones in moderate to excellent yields with t-BuOOH as oxidant under solvent-free conditions. Well deposition of Cu nanoparticles on the surface of SBA-15 support along with minimized diffusion limitations is a key factor for its high efficiency. The use of inexpensive, eco-friendly catalyst and operational simplicity offers the system attractive for large-scale applications.

#### References

- [1] S. Rochat, C. Minardi, J.Y. DeSaint Laumer, A.H. Herrmann, *Chimica Acta* 83 (2000) 1645–1671.
- [2] M. Hudlicky, *Oxidations in Organic Chemistry*, ACS Monograph No. 186, American Chemical Society, Washington DC, 1990.
- [3] R.A. Sheldon, J.K. Kochi, *Metal-catalyzed Oxidation of Organic Compounds*, Academic press, 1981. 318, (Chapter 10).
- [4] J. Muzart, A.N.A. Ajjou, *Journal of Molecular Catalysis* 66 (1991) 155–161.
- [5] J. Muzart, *Tetrahedron Letters* 28 (1987) 2131–2132.
- [6] P. Lei, H. Alper, *Journal of Molecular Catalysis* 61 (1990) 51–54.
- [7] M. Jurado-Gonzalez, A.C. Sullivan, J.R.H. Wilson, *Tetrahedron Letters* 44 (2003) 4283–4286.
- [8] N.H. Lee, C.S. Lee, D.S. Jung, *Tetrahedron Letters* 39 (1998) 1385–1388.
- [9] J.F. Pan, K. Chen, *Journal of Molecular Catalysis A: Chemical* 176 (2001) 19–22.
- [10] A.J. Catino, J.M. Nichols, H. Choi, S. Gottipamula, M.P. Doyle, *Organic Letters* 7 (2005) 5167–5170.
- [11] S. Murahashi, Y. Oda, T. Naota, T. Kuwabara, *Tetrahedron Letters* 34 (1993) 1299–1302.
- [12] M.D. Nikalje, A. Sudalai, *Tetrahedron* 55 (1999) 5903–5908.
- [13] S.I. Murahashi, N. Komiya, Y. Oda, T. Kuwabara, T. Naota, *The Journal of Organic Chemistry* 65 (2000) 9186–9193.
- [14] M. Gupta, S. Paul, R. Gupta, A. Loupy, *Tetrahedron Letters* 46 (2005) 4957–4960.
- [15] D.H.R. Barton, W. Chavasiri, *Tetrahedron* 50 (2005) 19–30.
- [16] S.S. Kim, K.S. Sar, P. Tamrakar, *Bulletin of the Korean Chemical Society* 23 (2002) 937–938.
- [17] D. Trong On, D. Desplandier-Giscard, C. Danumah, S. Kaliaguine, *Applied Catalysis A: General* 222 (2001) 299–357.
- [18] R.K. Jha, S. Shylesh, S.S. Bhoware, A.P. Singh, *Microporous and Mesoporous Materials* 95 (2006) 154–163.
- [19] H. Ma, J. Xu, C. Chen, Q. Zhang, J. Ning, H. Miao, L. Zhou, X. Li, *Catalysis Letters* 113 (2007) 104–108.
- [20] N. Anand, K.H.P. Reddy, G.V.S. Prasad, K.S.R. Rao, D.R. Burri, *Catalysis Communications* 23 (2012) 5–9.
- [21] T. Ohta, T. Tachiyama, K. Yoshizawa, T. Yamabe, T. Uchida, T. Kitakawa, *Inorganic Chemistry* 39 (2000) 4358–4369.
- [22] R. Maurya Mannar, Sweta Sikarwar, Trissa Joseph, Palanichamy Manikandan, S.B. Halligudi, *Reactive and Functional Polymers* 63 (2005) 71–83.
- [23] R. Maurya Mannar, Aarti Arya, Pedro Adao, Joao Costa Pessoa, *Applied Catalysis A: General* 351 (2008) 239–252.
- [24] Subbarayan Velusamy, T. Punniyamurthy, *Tetrahedron Letters* 44 (2003) 8955–8957.
- [25] T.H. Bennur, D. Srinivas, S. Sivasanker, *Journal of Molecular Catalysis A: Chemical* 207 (2004) 163–171.
- [26] D. Zhao, J. Feng, Q. Huo, N. Melosh, G.H. Fredrickson, B.F. Chmelka, G.D. Stucky, *Science* 279 (1998) 548–552.
- [27] S. Sreevardhan Reddy, D.R. Burri, A.H. Padmasri, P.K. Sai Prakash, K.S. Rama Rao, *Catalysis Today* 141 (2009) 61–65.
- [28] N. Anand, K.H.P. Reddy, K.S. Rama Rao, D.R. Burri, *Catalysis Letters* 141 (2011) 1355–1363.
- [29] N. Anand, K.H.P. Reddy, V. Swapna, K.S. Rama Rao, D.R. Burri, *Microporous and Mesoporous Materials* 143 (2011) 132–140.
- [30] G. Saidulu, N. Anand, K.S. Rama Rao, A. Burri, S.E. Park, D.R. Burri, *Catalysis Letters* 141 (2011) 1865–1871.
- [31] Z. Huang, F. Cui, H. Kang, J. Chen, X. Zhang, C. Xia, *Chemistry of Materials* 20 (2008) 5090–5099.
- [32] Y.-Y. Zhu, S.-R. Wang, L.-J. Zhu, X.-L. Ge, X.-B. Li, Z.-Y. Luo, *Catalysis Letters* 135 (2010) 275.
- [33] Z. Huang, F. Cui, J. Xue, J. Zuo, J. Chen, C. Xia, *Catalysis Today* 183 (2012) 42.
- [34] W.H. Tian, L.B. Sun, X.L. Song, X.Q. Liu, Y. Yin, G.S. He, *Langmuir* 26 (2010) 17398–17404.
- [35] R. Prasad, P. Singh, *Bulletin of Chemical Reaction Engineering & Catalysis* 6 (2011) 63–113.
- [36] S.B. Kumar, S.P. Mirajkar, G.C.G. Pais, P. Kumar, R. Kumar, *Journal of Catalysis* 156 (1995) 163–166.